Earth Surface Geochemistry and Mineralogy: Processes, Hazards, Soils, and Resources

Principal Author:
Wendy M. Calvin, University of Nevada, Reno, NV

Co-Authors (alphabetical):
Eyal Ben-Dor, Tel Aviv University, Tel Aviv, Israel
Janice Bishop, SETI Institute, Mountain View, CA
Joseph Boardman, AIG LLC, Boulder, CO
Roger N. Clark, Planetary Science Institute, CO
Tom Cudahy, CSIRO, Perth, Australia
Bethany L. Ehlmann, California Institute of Technology, Pasadena, CA
Robert O. Green, Jet Propulsion Laboratory, California Institute of Technology, Pasadena, CA
Bernard Hubbard, United States Geological Survey, Reston, VA
Raymond Kokaly, United States Geological Survey, Denver, CO
John Mars, United States Geological Survey, Reston, VA
John F. Mustard, Brown University, Providence, RI
Greg Okin, University of California, Los Angeles, CA
Cindy Ong, CSIRO, Australia
Roberto de Souza Filho, University of Campinas, Brazil
Freek van der Meer, ITC, Netherlands
Gregg Vane, Jet Propulsion Laboratory, California Institute of Technology, Pasadena, CA

Description: New spectroscopic measurements of the Earth's exposed surface to derive mineralogy are required to address key science and application targets. These measurements will advance understanding of fundamental geological processes, natural and anthropogenic hazards, soil geochemistry and evolution, and the location of energy and mineral resources.

Theme V: Earth Surface and Interior: Dynamics and Hazards
Core, mantle, lithosphere, and surface processes, system interactions, and the hazards they generate.

1. Science and Application targets

Fundamental questions about geologic processes, the natural resources that enable modern society to persist, and the ability to characterize and predict natural and anthropogenic hazards are closely tied to surface mineralogical composition and related physical properties. Yet the Earth's exposed rock and soil surface has been incompletely measured. Multiple community reports have determined that global compositional measurements are required to determine the link between surface-atmosphere interactions, biogeochemical cycles, and climate, tectonic, deep Earth, and surface processes [USGS 2007; NRC, 2007; 2010; 2012; NASA, 2014]. New comprehensive high quality measurements of the type successfully used for mapping the geochemistry and mineralogy of other planetary surfaces (e.g., Mars, Murchie et al., 2009; the Moon, Pieters et al., 2011; asteroids, De Sanctis et al., 2013) are urgently needed to close this gap. The science and applications targets identified below also directly address the goals stated in the 2007 Decadal Survey (NRC 2007) for understanding Earth surface changes, how the Earth supports life, and how human activities will impact future sustainability. ***A key element of "Theme V. Earth Surface: Dynamics and Hazards" is a suite of urgent science questions and applications that can be uniquely advanced with new comprehensive global measurement of the Earth's exposed surface mineralogy, geochemistry, and soil properties.*** This RFI response directly addresses this key element of Theme V.

1.1 New insights and constraints on fundamental geological processes

The composition of the Earth's surface preserves the fingerprint of coupled geodynamic, surface processes, and climate interactions that build and modify continental structures over a range of timescales. Plate margin evolution and dynamics, construction of continental scale stratigraphy, accumulation of economic resources, and associated geologic hazards and environmental impacts and sustainability derive from understanding these interactions. Some selected examples of the transformative nature of local mineralogical mapping done to date demonstrate discoveries that will be enabled with new accurate global surface mineral measurements of the Earth's exposed surface.

Fundamental programs in the earth sciences (NSF's GeoPRISMS, NASA's Earth Surface and Interior) are focused on the origin and evolution of continental crust, geochemical cycles, subsurface fluids and magmas and their interactions. Many regions have seen great benefits from application of remote mineral mapping (to date mostly from airborne instruments). For example, regional mineralogy mapping has provided new compositional basemaps for the interpretation of structural geological features, applied in reconstructing the fault offsets and lithologic controls on alluvial fan formation and erosion rates in Death Valley, extending field data taken in limited areas (Kruse, 2012). In the Oman ophiolite, orthopyroxene-rich cumulates, previously undocumented, were discovered using regional imaging spectroscopy and led to the promulgation of a new model for diapirism and creation of magma chambers in oceanic crust formation (Roy et al., 2008; Clenet et al., 2010). The spatial structure of compositional variation of ultramafic and metamorphic rocks in hard-to-access ancient continental cratons in Africa and Australia has also been mapped (e.g. Metelka et al., 2015; Rowan et al. 2005). In volcanic studies, remote sensing of mineralogy has provided crucial information for mapping and monitoring ash composition and flow history (e.g. Rocha-Lima et al., 2014; Wright et al. 2008; Guerrieri et al. 2015). Key ongoing areas of research informed by maps of mineralogy include the paleostructure of subduction zones and spreading ridges, and the mapping of fault zones to understand plate movement. Global mineral mapping at the tens of meters scale extends and connects isolated field measurements and vastly improves capabilities for differentiation of unit lithologies.

New comprehensive measurements to identify minerals and discriminate lithologies are required with the capability to distinguish carbonate and sedimentary facies, including fine variations in carbonate composition and clay mineralogy, map hydrothermal and metamorphic indicator minerals, and distinguish basaltic, andesitic, and mafic compositional suites.

1.2 Assessment and response to natural and anthropogenic hazards

Modeling of natural and anthropogenic Earth surface hazards is a fundamental goal of remote sensing, and as articulated in multiple community roadmaps compositional measurements are an imperative (NRC, 2007; USGS 2007). More precise surface compositional information is required to assess and mitigate hazards in advance of their occurrence, and to respond to hazards and disasters by classifying regions of highest priority for intervention and remediation.

For example, the likelihood of landslide hazards is critically dependent on the type and quantity of underlying bedrock and soils. Studies have previously used interferometry, textural analysis, or thermophysical properties to identify existing slides as well as incipient slides where the ground surface remains largely intact (e.g. Soeters and Van Westen, 1996; Whitworth et al., 2005; Metternicht et al., 2005). However new, accurate surface mineralogy is required to advance these efforts and distinguish dangerous swelling clays from similar phyllosilicates, which do not swell when wetted and hence pose less danger. Existing soil maps used in landslide models (e.g. Hong et al., 2007) are coarse scale and have to be interpolated to the finer scale of available topographic data. This results in a vast simplification of the spatial scale of true variability (e.g. Hubbard, 2015), particularly in vulnerable mountain environments where tectonically deformed geologic units vary over meters to hundreds of meters scale. Additionally, zones of localized hydrothermal mineralization pose special threat of debris flow creation because of their alteration to swelling clays (e.g. Ambers et al., 2001; Opfergelt et al., 2006). Imaging spectroscopy measurements in the Cascades have demonstrated detection of mineral zones with hazards not previously found in ground based surveys of the rugged, hard-to-access terrain (e.g. Crowley et al., 2003).

Additional hazard tracking and monitoring efforts have employed spectral mineral mapping to detect iron sulfates diagnostic of acid mine drainage and to map their extent in river catchments (Swayze et al., 2000; Choe et al., 2008; Riaza et al., 2011). The problems presented by the presence of asbestos, whether naturally occurring (Swayze et al., 2009) or in manmade construction materials on rooftops (Bassani, et al., 2007; Frassy et al., 2014) has been spatially mapped using imaging spectroscopy. Collection of high spectral resolution datasets have also been proposed for guiding remediation of residual contamination at brownfield sites (Slonecker and Fisher, 2014).

Advancing the science of Earth surface hazard monitoring requires the ability to accurately identify surface mineral constituents, map their distribution, and estimate their abundance. Key mineralogies are the smectite clays related to landslides and weak zones in volcanic terrain. Iron oxides and sulfates are important for natural and mine-related acid drainage hazards. Serpentine and dust source region mineral mapping can be used to assess and mitigate dust-related hazards. Space-based, accurate, uniform mineral maps would enable high-resolution inputs to hazard models to be applied globally, serving developing and advanced countries in a rapid and cost effective way.

1.3 Advance soil composition and process knowledge

Soil is a key element of the Earth's Critical Zone (NSF 2005). At present, global soil properties and mineral composition are poorly characterized. Earth system models rely on extrapolations from a database of fewer than 5000 samples globally (e.g., Claquin et al., 1999). Yet, soil properties revealed at the surface are fully accessible to assessment by remote sensing and indicate the processes that form soil as well as important underlying components (Whiting et al. 2006). The soil surface is exposed for observation in arid regions, tilled agricultural regions, and other zones where vegetation has been temporarily cleared. Comprehensive measurements of the Earth's exposed soil properties are needed as a baseline now and to initialize models to predict future trends in soil fertility and degradation.

The surface reflectance spectrum of soil is strongly tied to its mineralogy and particle size (Whiting et al. 2006; DeTar et al. 2008). These properties influence soil cation exchange capacity, which is an index of nutrient availability in soils, specific surface area, water holding capacity, and

response to mechanical disturbance, e.g., tillage, compaction from heavy machinery, grazing (Ben-Dor and Banin 1995). Key geochemical components of soil that influence surface reflectance include nutrients, e.g., Mg^{+2}, Ca^{+2}, K^{+}, N (Boggs et al. 2003), iron oxide and carbonate concentration, (e.g., Lagacherie et al. 2010), and also components related to salinity (Ben-Dor et al. 2002). The organic and clay components of soils influence cation exchange and water holding capacity and the formation of soil crusts (De Jong et al. 2009) that in turn influence soils' potential to act as a source or sink of atmospheric CO_2 (Bartholomeus et al. 2008; Gomez et al. 2008; Stevens et al. 2008; Stevens et al. 2010). Measurement of surface properties, e.g., mineralogy, moisture, organic carbon content can provide information on the formation and erosion of soils (Goldshleger et al. 2001; Lobell and Asner, 2001; Demattê and Nanni 2003; Ben-dor et al. 2004; Ben-Dor et al. 2006; Galvão et al. 2008). Among the important large-scale changes that humans make to soils is salinization, a major form of soil degradation worldwide. Surface geochemical and reflectance signatures can reveal levels of soil salinization (Dehaan and Taylor 2002; Dehaan and Taylor 2003).

To advance soil science, new measurement of the surface composition of arid lands, fallow fields, sparsely vegetated, and temporarily cleared areas are required to update global soil databases with uniformly measured mineralogical information and to provide estimate of iron oxide, clay, organic carbon, carbonate, and salinity metrics for input into geochemical, vegetation, carbon cycling, and radiative forcing models.

1.4 Surface Resource Identification and Policy Support

Increased demand for limited resources requires an immediate and comprehensive assessment of the exposed surface mineralogy of the Earth, which provides a key window into the potential available new resources as well as a baseline for resources currently being extracted (Rowan et al., 1995, Sabins 1999, Kruse 2012, Kruse et al., 2012, Swayze et al., 2014, Calvin and Pace, 2016). However, a global inventory of resources using surface mineral composition as a key indicator of available resources does not yet exist. In this context, resources include both mineral resources, e.g., precious and base metals, aggregates, and building materials, energy resources in conventional and unconventional hydrocarbons, and renewable geothermal energy. Global strategic areas include development of raw material inventories, monitoring development, assessment of future resource demand, and balancing development with environmental impacts and human health hazards associated with resource extraction. This requires accurate and comprehensive measurement of mineralogy exposed at the surface. Despite potential for mineral development, many remote areas remain largely under-explored. Mineral mapping, primarily with airborne measurements, has occurred in remote and vegetated regions such as Greenland and Alaska (Bedini, 2011; Hoefen et al. 2015), over large regional areas such as Afghanistan and the Western USA (Kokaly et al. 2011, 2013; Mars, 2011; Rockwell and Hofstra, 2008). Remotely sensed imaging enabled mineral resource assessment in war-torn Afghanistan where traditional field mapping was a potentially deadly undertaking (King et al., 2012).

New global measurements of the exposed surface that allow detail characterization of hydrothermal alteration suites, temperature dependent mineralogy, and features associated with hydrocarbons are required.

2. Utility of the measured variables.

The targets identified in the previous sections can be addressed with new comprehensive measurements of the Earth's exposed surface mineralogy and geochemistry. Compounds exposed at the Earth's surface absorb and scatter light differently across the visible and infrared portions of the spectrum due to their molecular/crystal/structural properties (e.g., Clark, 1999). Thus, the interaction of light with matter recorded in a contiguous spectral measurement provides the ability to detect, identify, and quantify the surface mineralogy required to achieve the needed science targets described above.

Figure 1 shows an example of the spectral signatures for ten relevant Earth surface minerals as full spectra from 400 to 2500 nm (0.4 to 2.5 μm). Also shown are the spectra convolved to the Landsat thematic mapper bands. A full spectral measurement at high spectral resolution is required to deconvolve the effects of the atmosphere, distinguish between important minerals with similar signatures, and quantify contributions from multiple materials given overlapping signatures (e.g. Swayze et al., 2003, Clark et al., 2003; 2014). The utility of this spectroscopic approach for measuring the Earth's surface was identified in the NRC's last Decadal Survey (NRC 2007) and Landsat and Beyond report (NRC 2013).

Algorithms to extract geochemistry and mineralogy from measured spectra are well advanced, being based on more than 20 years of high quality airborne imaging spectrometer measurements of the Earth's surface. Figure 2 shows a spectral fitting method (Clark et al., 2003) to identify the clay mineral kaolinite at Cuprite, NV. Figure 3 shows a recent mosaic of the Salton Sea, CA region with several diagnostic mineral signatures. This was measured by AVIRIS as part of a campaign to simulate data sets of the 2007 Decadal Tier 2 mission HyspIRI (Lee et al., 2015). Figure 4 shows compositional maps generated using spectral feature fitting. The region includes the science and applications targets identified here. The detailed geochemistry and gradients revealed provide insight into related tectonic processes along the San Andreas fault (e.g. fault offset, fluid alteration). Landslide risk as related to mineral composition in steep terrain can be assessed (Hubbard 2015). The Salton Sea region is a known mineral dust source hazard area, and the surface composition of exposed shorelines can be used to constrain models and predict risks. The soil composition of the fallow agricultural fields and adjacent lands are measured, and repeat acquisition can capture different fields with exposed soil for comprehensive mapping. Information on current mining activities and potential future mineral resource extraction is revealed through identification of alteration mineral exposures. This example from airborne measurements demonstrates the approach that would be used to address science and applications targets globally for the exposed terrestrial surface of the Earth.

3. Key requirements for achieving the science and application targets

As discussed in Section 1, these targets require the identification of a variety of discrete minerals and lithologies with sufficient spectral and spatial resolution to map their distribution and estimate their abundance. This includes numerous metamorphic indicator minerals; basaltic, andesitic, and mafic compositional suites; swelling clays (smectites) and serpentine (asbestiform) minerals; characteristic hydrothermal alteration suites; temperature dependent mineralogy; and features associated with hydrocarbons. For assessing acid generation potential, measurement of iron oxide and select sulfate minerals is required. To advance soil science, measurement of the composition of arid lands, fallow fields, and sparsely vegetated regions to update global soil classifications with quantitative mineralogical information and provide estimates of iron, clay, organic carbon, carbonate, and salinity metrics is required. ***All these surface materials and mineral assemblages have well-known, diagnostic spectral absorption features.***

The requirements and their links to the science and applications targets are shown in Table 1. The spectral range and sampling required is from 400 to 2500 nm with ≤10 nm sampling. These spectral requirements are derived from multiple studies (e.g. Clark 1999, Clark et al., 2003, Clark et al., 2014) and a detailed analysis examining spectral characteristics versus signal-to-noise ratio (Swayze et al., 2003) to detect the phases noted above. This spectral range also contains the atmospheric features to allow automated atmospheric correction (Gao et al., 1993, 2009, Thompson et al., 2015, 2016). The radiometric range of the spectral measurements must span from dark to bright materials exposed on the Earth's surface. The radiometry of the measurements must account for the solar illumination, two-way transmittance of the atmosphere and the reflectance properties of the material. Figure 5 shows the reference top of atmosphere radiance from a 0.05, 0.25, 0.75 reflectance surface with solar illumination

at 45° modeled with MODTRAN and a predicted signal-to-noise ratio (SNR) consistent with mapping ≥90% of the minerals (Swayze et al., 2003). The reference SNR is also well above that achieved by the existing NASA Hyperion instrument (Ungar et al, 2003, Middleton et al., 2013), a technology demonstration that was shown to be broadly capable of mapping surface mineralogy (Cudahy et al., 2001, Kruse et al., 2003, Gersman et al., 2008, Chudnovsky, et al., 2009, Clark et al., 2011) though it was limited by a 7.5 km swath, restricted on-board storage, and downlink.

The spatial sampling requirement is ≤30 m nadir to provide access to high fractional concentration of constituents of interest with sufficient SNR for identification and abundance assessment. Spatial sampling of 30 m also provides continuity with Landsat and related multi-spectral measurements. A swath width of ≥90 km provides sufficient temporal sampling to capture cloud free observation over ≥75% of the terrestrial surface in a year based on refined cloud analysis from MODIS observations (Mercury et al., 2010). This would provide full terrestrial imaging every 32 days. Over two years, ≥85% of the terrestrial surface where surface mineral and soils are exposed will be measured. A goal swath to provide repeat coverage every 16 days could also be implemented to match Landsat frequency. To enhance the disaster response capability, the measurement should include a pointing capability to target specific areas of interest within 3 days of designation.

4. Near Term Success and Affordability

The spectral measurements described above can be achieved affordably in the coming decade, because of the investments that were made in response to the global terrestrial and coastal observing missions that were outlined in the 2007 Decadal Survey (NRC 2007), the Landsat and Beyond report (NRC 2013), and other studies. These measurements would build on a legacy of airborne and spaceborne instruments including airborne: AIS (Vane et al, 1984), AVIRIS (Green et al., 1998), and AVIRIS-NG (Hamlin et al., 2011) and space: NIMS (Carlson et al., 1992), VIMS (Brown et al., 2004), Deep Impact (Hampton et al., 2005), CRISM (Murchie et al., 2007), EO-1 Hyperion (Ungar et al, 2003, Middleton et al., 2013), M3 (Green et al., 2011) and MISE (now in development for Europa).

NASA-guided engineering studies in 2014 and 2015 validated that a Landsat-class VSWIR imaging spectrometer instrument (380 to 2510 nm @ ≤10 nm sampling, Figure 6) with a 185 km swath, 30 m spatial sampling and 16 day revisit with high signal-to-noise ratio and the required spectroscopic uniformity, can be implemented affordably for a three year mission. It would have a mass of <100 kg), require about 100 W of power), and fill a volume that is compatible with a Pegasus class launch or ride share (Figure 7). The telescope can be adapted to higher orbits. Such an instrument would provide global 16-day repeat coverage, while airborne equivalent measurements would take >10 years and cost >$1 billion. Additionally, much airspace is restricted or otherwise inaccessible making complete global coverage impossible. The key to these measurements is an optically fast spectrometer providing high SNR designed to accommodate the full spectral and spatial ranges (Mouroulis et al., 2016). A scalable prototype F/1.8 full VSWIR spectrometer (van Gorp et al., 2014) has been developed, aligned, and is being qualified (Figure 8). Data rate and volume challenges have been addressed by development and testing of a lossless compression algorithm for spectral measurements (Klimesh et al., 2006, Aranki et al., 2009ab, Keymeulen et al., 2014). The algorithm is now a CCSDS standard (CCSDS 2015). With compression and the current Ka band downlink offered by KSAT and others, all terrestrial/coastal measurements can be downlinked (Figure 9). Algorithms for calibration (Green et al., 1998) and atmospheric correction (Gao et al., 1993, 2009, Thompson et al., 2015, 2016) of large diverse data sets have been benchmarked as part of the HyspIRI preparatory campaign (Lee et al., 2015), the AVIRIS-NG India and Greenland campaigns, and other campaigns. There is good potential for international partnerships that would reduce the cost to NASA and accelerate the availability of the measurements.

Science and Applicaitons Target	Objectives	Physical Parameter	Observable	Measurement Requirements	Other Measurement Characteristics
V. Earth Surface and Interior: Dynamics and Hazards: Core, mantle, lithosphere, and surface processes, system interactions, and the hazards they generate. **Earth Surface Geochemistry and Mineralogy for Geologic Processes, Hazards, Soils, and Resources**	O1. New insights and constraints on fundamental geological processes O2. Assessment and response to natural and anthropogenic hazards O3. Advance soil composition and process knowledge O4. Surface Resource Identification and Policy Support	Occurrence and fractional abundance estimate (0-1.0 with uncertainty) of minerals and geochemicals expressed at exposed surface: • Iron oxides • Sulfates • Clays • Carbonates • Amphiboles • Mafic minerals • Hydrocarbons Estimation of confounding factors: • Fractional surface cover for green and non-photosynthetic vegetation • Water vapor, cirrus clouds, and aerosols	Spectral reflectance of the exposed surface from atmospherically corrected top of atmosphere spectral radiance	Spectral • 450 to 2450 nm range • ≤ 10 nm sampling • ≤ 15 nm FWHM • ≤ 1 nm calibraiton uncertainty Radiometric • 0 to max Lambert range • 99% linear of 5 to 95 % of range • SNR see figures 5, 6 • ≤ 5% calibraiton uncertainty Spatial • ≥ 90 km swath • ≤ 30 m sampling • ≤ 30 m 1σ uncertainty Uniformity • ≤10% cross-track spectral variation • ≤10% spectral IFOV variation	Sun synchronous ~11am crossing for good illumination and prior to cloud build up. Cloud free measurement for ≥ 80% terrestrial exposed surface. At least two years of measurement for capture of seasonal low vegetation states and fallow agricultural fields. Pointable for 3 day revisit for event response.

Table 1. The detailed traceability from science and applications targets to physical parameters, to observables, and to measurement requirements has been enabled by over a decade of imaging spectroscopy observations of the Earth, the Moon, Mars and other bodies in the Solar System.

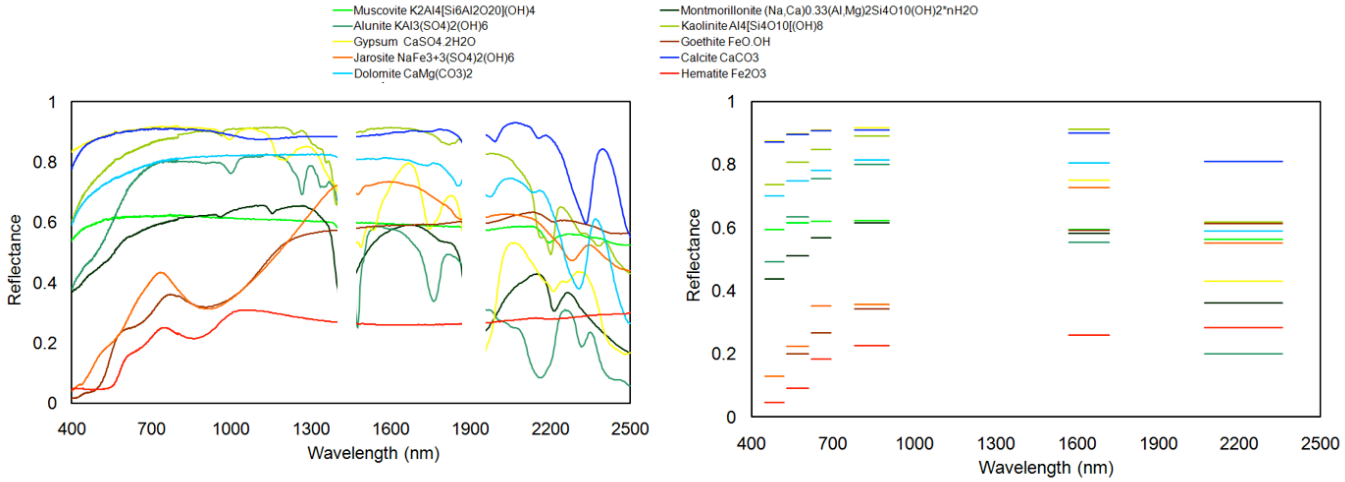

Figure 1. (left) Ten mineral reflectance spectra showing the diversity of absorption and scattering signatures tied to composition available for measurement in the 400 to 2500 nm region of the spectrum. Acquisition of such data enables highly accurate identification of Earth surface materials and assessment of their abundances. (right) The same mineral spectra convolved to the Landsat TM bands showing the loss of spectroscopic information required for unambiguous identification and abundance estimation. The broad-band sampling provided by the TM bands limits the analysis of the data largely to the relative brightness within each of the bands. Brightness is complicated by sun angle, slope effects, shading, and other factors. The utility of imaging spectroscopy is thus greatly enhanced over broad-band multispectral imaging.

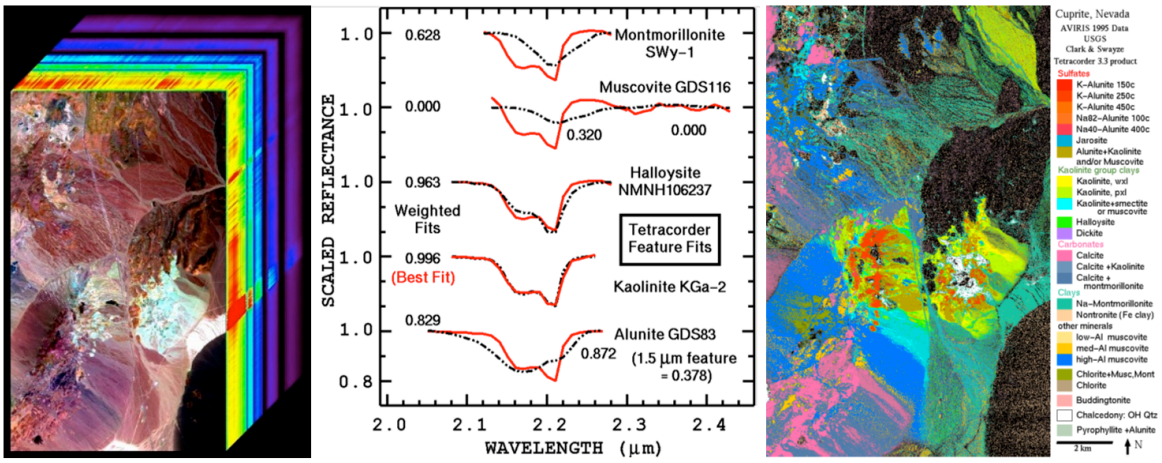

Figure 2. (left) Airborne imaging spectrometer data set over Cuprite,NV. (center) Spectral feature fitting algorithm to detect and identify minerals based on their measured spectrum and the spectral signatures of known minerals from a spectral library. (right) Surface compositional map derived from spectroscopic signatures. It is maps of this type that are required on a global scale. Global coverage can only be achieved in any practical sense from Earth orbit.

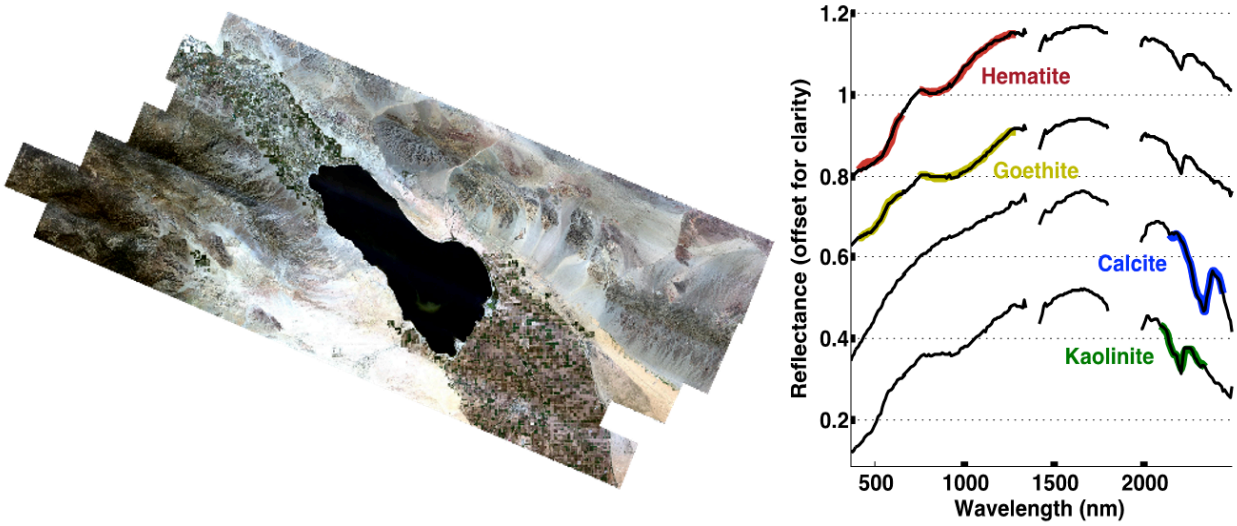

Figure 3. (left) Approximate natural color mosaic of a 2014 airborne imaging spectrometer data set over the Salton Sea region, CA. (right) Example spectral fits for surface mineralogy mapping from calibrated and atmospherically corrected spectra.

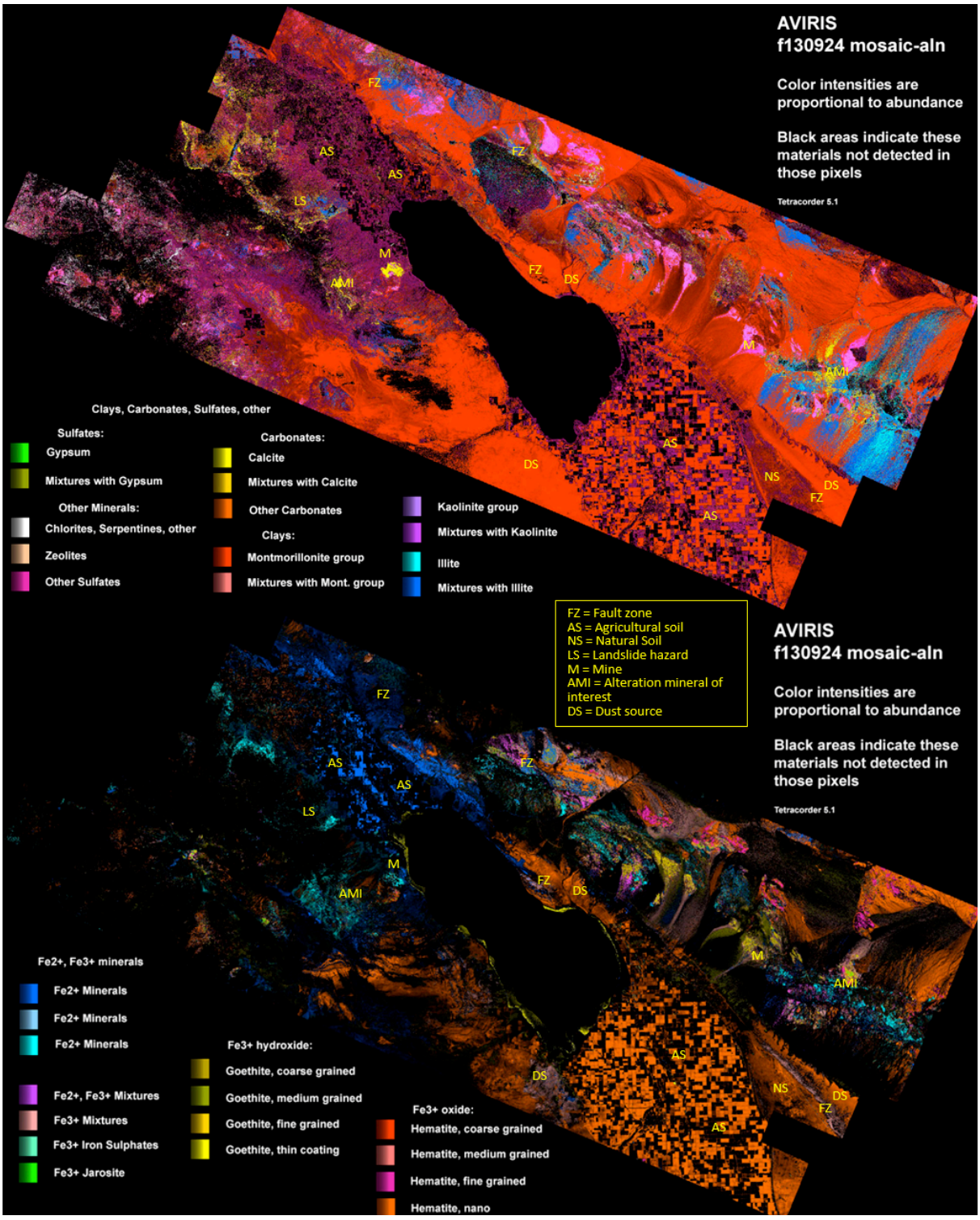

Figure 4. Surface mineral and soil maps from spectral fitting to airborne imaging spectrometer measurements of the Salton Sea Region, CA. (top) Clay, carbonate and other alteration minerals of interest. (bottom) Iron oxide and related minerals. This area of the Earth's surface demonstrates the multitude of science and application targets that can be easily addressed with this type of data.

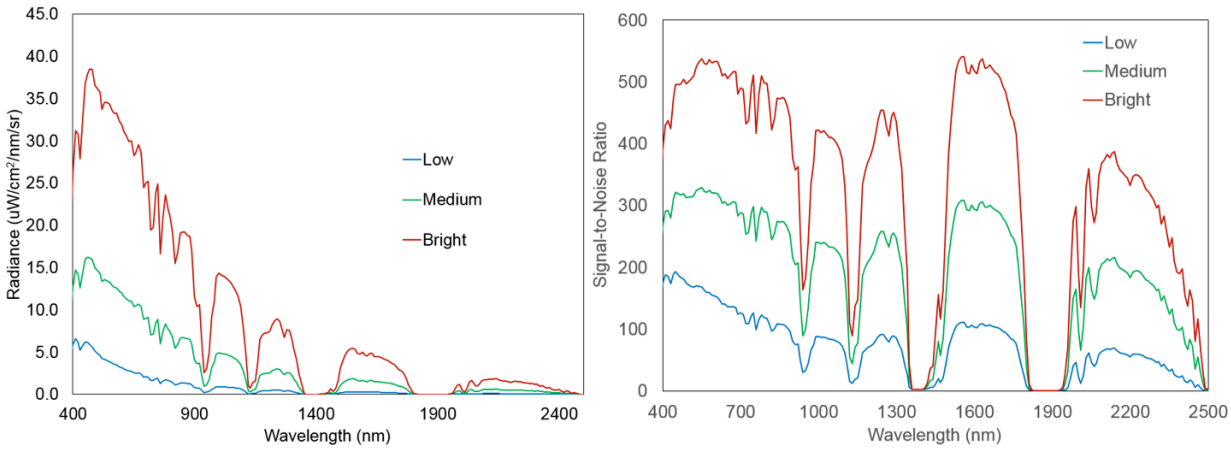

Figure 5. (left) Reference radiances for surface materials of 0.05, 0.25 and 0.75 reflectance illuminated at 45° through the standard mid latitude summer atmosphere. (right) Signal-to-noise ratios for the reference radiances that enable accurate surface mineral/composition and abundance estimation to achieve the designated Earth surface science and applications targets.

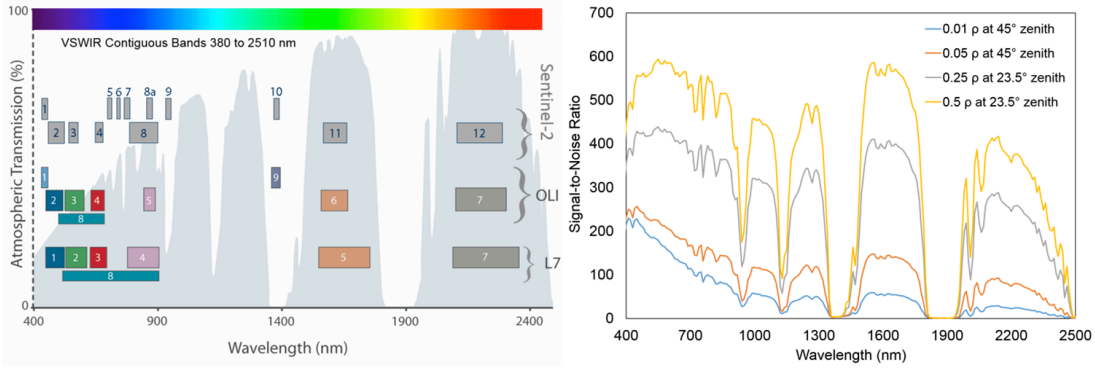

Figure 6. (left) The Landsat and Sentinal-2 bands created by summing the narrow VSWIR spectral channels demonstrate the straightforward manner with which data continuity can be maintained with heritage multispectral data sets while utilizing the advanced capability of a full spectrum measurement from 380 to 2510 nm. (right) Signal-to-noise ratio for 30 m sampling with F/1.8 VSWIR Dyson imaging spectrometer for a range of reference radiances. These are actual measured data acquired with a mature engineering model of the Dyson spectrometer. The next step for the instrument is the spaceflight unit.

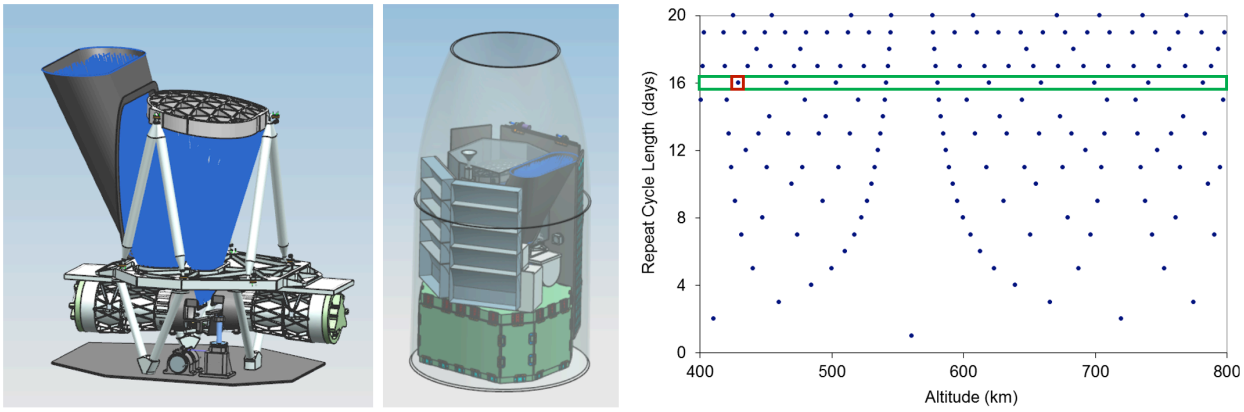

Figure 7. (left) Opto-mechanical configuration with one telescope feeding two field split wide swath F/1.8 VSWIR Dyson spectrometer providing 185 km swath and 30 m sampling. (center) Imaging spectrometer with spacecraft (248 kg, 670 W with margin) configured for launch in a Pegasus shroud for an orbit of 429 km altitude, 97.14 inclination to provide 16 day revisit for three years. (right) Orbital altitude and repeat options showing an altitude of 429 km with a fueled spacecraft supports the three year mission with the affordable Pegasus launch. Higher orbits are viable with a larger launch vehicle.

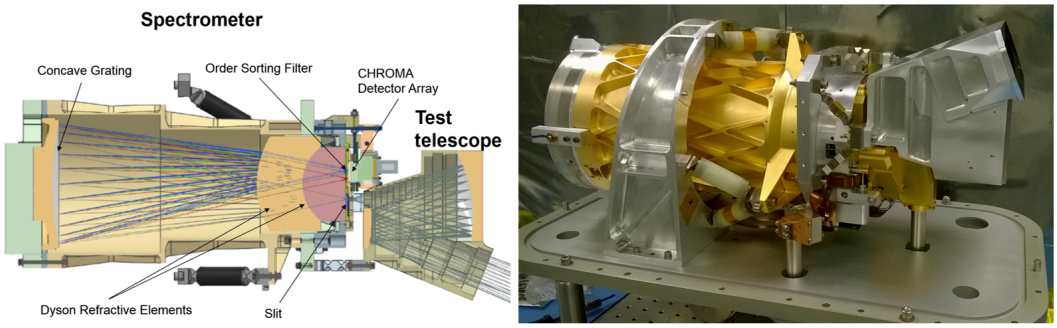

Figure 8. Design of a wide swath F/1.8 VSWIR Dyson covering the spectral range from 380 to 2510 nm. (right) Dyson imaging spectrometer in qualification that uses a full spectral range HgCdTe detector array.

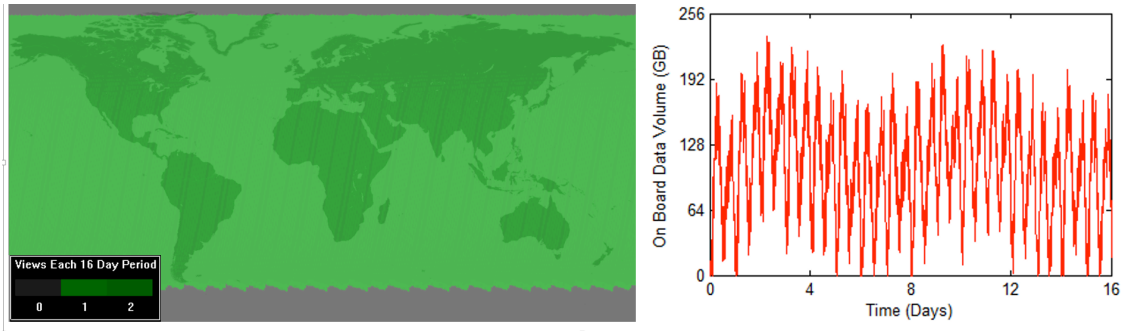

Figure 9. (left) Potential illuminated surface coverage every 16 days for the surface of the Earth. (right) On-board data storage usage for illuminated terrestrial/coastal regions with downlink using Ka Band (<900 mb/s) to KSAT Svalbard and Troll stations. Oceans and ice sheets can be spatially averaged for downlink.

References

Ambers, RKR, (2001) Relationships between clay mineralogy, hydrothermal metamorphism, and topography in a Western Cascades watershed, Oregon, USA. Geomorphology 38, 47–61.

Aranki, N., A. Bakshi, D. Keymeulen, and M. Klimesh (2009a). Fast and adaptive lossless onboard hyperspectral data compression system for space applications, 2009 IEEE Aerospace Conf., 7-14 March. doi:10.1109/AERO.2009.4839534.

Aranki, N., D. Keymeulen, A. Bakshi, and M. Klimesh (2009b). Hardware implementation of lossless adaptive and scalable hyperspectral data compression for space, NASA ESA Conf. Adap. Hardware Sys., 29 July – 1 Aug. doi:10.1109/AHS.2009.66.

Bartholomeus, H.M., Schaepman, M.E., Kooistra, L., Stevens, A., Hoogmoed, W.B., & Spaargaren, O.S.P. (2008). Spectral reflectance based indices for soil organic carbon quantification. *Geoderma, 145*, 28-36

Bassani, C. et al. (2007) Deterioration status of asbestos-cement roofing sheets assessed by analyzing hyperspectral data. Remote Sensing of Environment, 109, 3, 361-378.

Bedini, E. (2011), Mineral mapping in the Kap Simpson complex, central east Greenland, using HyMap and ASTER remote sensing data, *Advances in Space Research*, *47*, 60-73, doi:10.1016/j.asr.2010.08.021.

Ben-Dor, E., & Banin, A. (1995). Near-Infrared Analysis as a Rapid Method to Simultaneously Evaluate Several Soil Properties. *Soil Science Society of America Journal, 59*, 364-372.

Ben-Dor, E., Chabrillat, S., Demattê, J.A.M., Taylor, G.R., Hill, J., Whiting, M.L., & Sommer, S. (2009). Using Imaging Spectroscopy to study soil properties. *Remote Sensing Of Environment, 113, Supplement 1*, S38-S55

Ben-dor, E., Goldshleger, N., Braun, O., Kindel, B., Goetz, A.F.H., Bonfil, D., Margalit, N., Binaymini, Y., Karnieli, A., & Agassi, M. (2004). Monitoring infiltration rates in semiarid soils using airborne hyperspectral technology. *International Journal of Remote Sensing, 25*, 2607-2624

Ben-Dor, E., Levin, N., Singer, A., Karnieli, A., Braun, O., & Kidron, G.J. (2006). Quantitative mapping of the soil rubification process on sand dunes using an airborne hyperspectral sensor. *Geoderma, 131*, 1-21

Ben-Dor, E., Patkin, K., Banin, A., & Karnieli, A. (2002). Mapping of several soil properties using DAIS-7915 hyperspectral scanner data-a case study over clayey soils in Israel. *International Journal of Remote Sensing, 23*, 1043-1062

Boggs, J.L., Tsegaye, T., Coleman, T.L., Reddy, K., & Fahsi, A. (2003). Relationship between hyperspectral reflectance, soil nitrate-nitrogen, cotton leaf chlorophyll, and cotton yield: a step toward precision agriculture. *Journal of Sustainable Agriculture, 22*, 5-16Brown et al., 2004

Brown, R. H., et al. (2004) The Cassin Visual and Infrared Mapping Spectrometer (VIMS) Investigation.," Space Science Reviews 115: 111–168, 2004

Calvin, Wendy M., and Elizabeth L. Pace. (2016) Utilizing HyspIRI Prototype Data for Geological Exploration Applications: A Southern California Case Study. Geosciences 6: p.14.

Carlson, R. W., Weissman, P. R., Smythe, W. D., & Mahoney, J. C., (1992) Near-Infrared Mapping Spectrometer experiment on Galileo, Space Science Reviews (ISSN 0038-6308), 60 (1-4), p. 457-502.

CCSDS, "LOSSLESS MULTISPECTRAL AND HYPERSPECTRAL IMAGE COMPRESSION INFORMATIONAL REPORT," CCSDS 120.2-G-1, GREEN BOOK, 2015, http://public.ccsds.org/publications/archive/120x2g1.pdf

Choe E. et al., (2008) Mapping of heavy metal pollution in stream sediments using combined geochemistry, field spectroscopy, and hyperspectral remote sensing: A case study of the Rodalquilar mining area, SE Spain. Remote Sensing of Environment 112 3222–3233.

Chudnovsky, A., et al. (2009) Mineral content analysis of atmospheric dust using hyperspectral information from space." Geophysical Research Letters 36.15.

Claquin, T., M. Schulz, and Y. J. Balkanski (1999), Modeling the mineralogy of atmospheric dust sources, *Journal of Geophysical Research-Atmospheres*, *104*(D18), 22243-22256, doi:10.1029/1999jd900416.

Clark, R.N., **(**1999) Chapter 1: Spectroscopy of Rocks and Minerals and Principles of Spectroscopy, Manual of Remote Sensing, (A.N. Rencz, ed.) John Wiley and Sons, New York, p 3-58, 1999. Online at: http://speclab.cr.usgs.gov/PAPERS.refl-mrs/

Clark, R.N., Swayze, G.A., Livo, K.E., Kokaly, R.F., Sutley, S.J., Dalton, J.B., McDougal, R.R., and Gent, C.A., (2003) Imaging spectroscopy: Earth and planetary remote sensing with the USGS Tetracorder and expert systems, Journal of Geophysical Research, Vol. **108**(E12), 5131, doi:10.1029/2002JE001847, p. 5-1 to 5-44, December, 2003. http://speclab.cr.usgs.gov/PAPERS/tetracorder

Clark, R.N., Swayze, G.A., Leifer, I. Livo, K.E., Kokaly, R., Hoefen, T., Lundeen, S., Eastwood, M., Green, R.O., Pearson, N., Sarture, C., McCubbin, I., Roberts, D., Bradley, E., Steele, D., Ryan, T., Dominguez, R., and the Air borne Visible/Infrared Imaging Spectrometer (AVIRIS) Team, (2010) A method for quantitative mapping of thick oil spills using imaging spectroscopy: U.S. Geological Survey Open-File Report 20101167, 51 p. http://pubs.usgs.gov/of/2010/1167/

Clark, R.N., and Wise, R.A. (2011) Mapping with imaging spectroscopy, Fort Cobb Reservoir watershed, southwestern Oklahoma, Chapter 6 of Becker, C.J., ed., Assessment of conservation practices in the Fort Cobb Reservoir watershed, southwestern Oklahoma: U.S. Geological Survey Scientific Investigations Report 2010-5257, 23 p. http://pubs.usgs.gov/sir/2010/5257/Chapter6.pdf

Clark, R. N., G. A Swayze, R. Carlson, W. Grundy, and K. Noll (2014) Spectroscopy from Space, Chapter 10 in Spectroscopic Methods in Mineralogy and Material Sciences, Reviews in Mineralogy & Geochemistry, Grant Henderson, ed, Mineralogical Society of America 78, 399-446.

Clenet, H et al., (2010) Thick sections of layered ultramafic cumulates in the Oman ophiolite revealed

by an airborne hyperspectral survey: Petrogenesis and relationship to mantle diapirism. Lithos, 114, 265-281.

Crowley, James K., and David R. Zimbelman. (1997) Mapping hydrothermally altered rocks on Mount Rainier, Washington, with airborne visible/infrared imaging spectrometer (AVIRIS) data. Geology 25.6: 559-562.

Crowley, J.K., Hubbard, B.E., Mars, J.C. Analysis of potential debris flow source areas on Mount Shasta, California, by using airborne and satellite remote sensing data. Remote Sensing of Environment, 87, 2-3, 345-358, 2003.

Cudahy, T. J., et al. (2001) The performance of the satellite-borne Hyperion Hyperspectral VNIR-SWIR imaging system for mineral mapping at Mount Fitton, South Australia." Geoscience and remote sensing symposium, 2001. IGARSS'01. IEEE 2001 International. Vol. 1. IEEE.

Cudahy, T. et al. (2016) Satellite-derived mineral mapping and monitoring of weathering, deposition and erosion. Scientific Reports 6, Article number: 23702, doi:10.1038/srep23702

De Jong, S.M., Addink, E.A., Van Beek, R., & Duijsings, D. (2009). Mapping of soil surface crusts using airborne hyperspectral HyMap imagery in a Mediterranean environment. *Anais XIV Simpósio Brasileiro de Sensoriamento Remoto*, 25-30

De Sanctis, M. C., et al. (2013), Vesta's mineralogical composition as revealed by the visible and infrared spectrometer on Dawn, *Meteoritics & Planetary Science*, *48*(11), 2166-2184, doi:10.1111/maps.12138.

Dehaan, R., & Taylor, G.R. (2003). Image-derived spectral endmembers as indicators of salinisation. *International Journal of Remote Sensing, 24*, 775-794

Dehaan, R.L., & Taylor, G.R. (2002). Field-derived spectra of salinized soils and vegetation as indicators of irrigation-induced soil salinization. *Remote Sensing Of Environment, 80*, 406-417

Demattê, J.A.M., & Nanni, M.R. (2003). Weathering sequence of soils developed from basalt as evaluated by laboratory (IRIS), airborne (AVIRIS) and orbital (TM) sensors. *International Journal of Remote Sensing, 24*, 4715-4738

DeTar, W.R., Chesson, J.H., Penner, J.V., & Ojala, J.C. (2008). Detection of soil properties with airborne hyperspectral measurements of bare fields. *Transactions of the ASABE, 51*, 463-470Frassy et al., 2014

Frassy, F. et al. (2014) Mapping Asbestos-Cement Roofing with Hyperspectral Remote Sensing over a Large Mountain Region of the Italian Western Alps. Sensors, 14, 15900-15913.

Galvão, L.S., Formaggio, A.R., Couto, E.G., & Roberts, D.A. (2008). Relationships between the mineralogical and chemical composition of tropical soils and topography from hyperspectral remote sensing data. *Isprs Journal of Photogrammetry and Remote Sensing, 63*, 259-271

Gao, B.-C., K. Heidebrecht, and A. Goetz (1993). Derivation of scaled surface reflectances from

AVIRIS data, Remote Sens. of Environ., 44, 165-178. doi:10.1016/0034- 4257(93)90014-O.

Gao, B.-C., M. Montes, C. Davis, and A. Goetz (2009). Atmospheric correction algorithms for hyperspectral remote sensing data of land and ocean, Remote Sens. of Environ., 113, 17-24. doi:10.1016/j.rse.2007.12.015.

Gersman, Ronen, et al. (2008) Mapping of hydrothermally altered rocks by the EO-1 Hyperion sensor, Northern Danakil Depression, Eritrea." International Journal of Remote Sensing 29.13: 3911-3936.

Goldshleger, N., Ben-Dor, E., Benyamini, Y., Agassi, M., & Blumberg, D.G. (2001). Characterization of soil's structural crust by spectral reflectance in the SWIR region (1.2–2.5 μm). *Terra Nova, 13*, 12-17

Gomez, C., Viscarra Rossel, R.A., & McBratney, A.B. (2008). Soil organic carbon prediction by hyperspectral remote sensing and field vis-NIR spectroscopy: An Australian case study. *Geoderma, 146*, 403-411

Green, Robert O., et al. (1998) Imaging spectroscopy and the airborne visible/infrared imaging spectrometer (AVIRIS). Remote Sensing of Environment 65.3: 227-248.

Green, R. O., et al. (2011) The Moon Mineralogy Mapper (M3) imaging spectrometer for lunar science: Instrument description, calibration, on-orbit measurements, science data calibration and on-orbit validation. Journal of Geophysical Research: Planets 116.E10.

Guerrieri, L., L. Merucci, S. Corradini, and S. Pugnaghi (2015), Evolution of the 2011 Mt. Etna ash and SO2 lava fountain episodes using SEVIRI data and VPR retrieval approach, *Journal of Volcanology and Geothermal Research*, *291*, 63-71, doi:10.1016/j.jvolgeores.2014.12.016.

Hamlin, L., et al. (2011) Imaging spectrometer science measurements for terrestrial ecology: AVIRIS and new developments." Aerospace Conference, IEEE, p. 1-7.

Hampton, Donald L., et al. (2005) An overview of the instrument suite for the Deep Impact mission. Space Science Reviews 117.1-2: 43-93.

Hoefen, T. M. et al. (2015) Characterizing geology and mineralization at high latitudes in Alaska using airborne and field-based imaging spectrometer data. American Geophysical Union Fall Meeting, 2015, AGU 2015 Fall Meeting, abstract GC23K-1231.

Hong, Y., Adler, R. & Huffman, G. (2007) Use of satellite remote sensing data in the mapping of global landslide susceptibility. Nat. Hazards. 43, 245–256.

Hubbard, Bernard. (2015) Field, Laboratory and Imaging spectroscopic Analysis of Landslide, Debris Flow and Flood Hazards in Lacustrine, Aeolian and Alluvial Fan Deposits Surrounding the Salton Sea, Southern California. American Geophysical Union Fall Meeting, abstract GC23K-1229.

Keymeulen, D., N. Aranki, A. Bakhshi, H. Luong, C. Sarture, D. Dolman (2014). Airborne Demonstration of FPGA implementation of Fast Lossless Hyperspectral Data Compression System, Adap. Hard. Sys. Conf., 278-284. doi:10.1109/AHS.2014.6880188.

King, T.V.V., Kokley, R.F., Hoefen, T.M., and Johnson, M.R. (2012). Hyperspectral remote sensing data maps minerals in Afghanistan: Eos, 93(34), 325-326.

Klimesh, M. (2006). Low-Complexity Adaptive Lossless Compression of Hyperspectral Imagery, Proc. SPIE Optics & Photonics Conference, 6300, 9. doi:10.1117/12.682624.

Kokaly, R. F., King, T. V. V., Hoefen, T. M., Dudek, K. B., & Livo, K. E. (2011). Surface materials map of Afghanistan: carbonates, phyllosilicates, sulfates, altered minerals, and other materials: US Geological Survey Scientific Investigations Map 3152–A, one sheet, scale 1: 1,100,000. Also available at http://pubs. usgs. gov/sim/3152/A.

Kokaly, R.F., King, T.V.V., and Hoefen, T.M. (2013). Surface mineral maps of Afghanistan derived from HyMap imaging spectrometer data, version 2: U.S. Geological Survey Data Series 787, 29 p., http://pubs.usgs.gov/ds/787/.

Kruse, FA, JW Boardman, and JF Huntington. (2003) Comparison of airborne hyperspectral data and EO-1 Hyperion for mineral mapping. Geoscience and Remote Sensing, IEEE Transactions on 41.6: 1388-1400.

Kruse, Fred A. (2012) Mapping surface mineralogy using imaging spectrometry. Geomorphology 137.1: 41-56.

Kruse, Fred A., et al. (2012) Mapping alteration minerals at prospect, outcrop and drill core scales using imaging spectrometry. International journal of remote sensing 33.6: 1780-1798.

Lagacherie, P., Gomez, C., Bailly, J.S., Baret, F., & Coulouma, G. (2010). The use of hyperspectral imagery for digital soil mapping in mediterranean areas. *Digital Soil Mapping* (pp. 93-102): Springer

Lee, Christine M., et al. (2015) An introduction to the NASA Hyperspectral InfraRed Imager (HyspIRI) mission and preparatory activities. Remote Sensing of Environment 167: 6-19.

Lobell, DB and GP Asner. (2001) Moisture Effects on Soil Reflectance. Soil Science Society of America Journal, 66(3), 722-727.

Mars, J. (2011) Regional mapping methods using ASTER data to map minerals in the U.S. Basin and Range, (U. S. Geological Survey, Reston, VA, United States) Source: American Geophysical Union Fall Meeting, 2011, American Geophysical Union 2011 Fall Meeting, abstract #V11C-2527.

Mercury, M., R. Green, S. Hook, B. Oaida, W. Wu, A. Gunderson, and M. Chodas (2012), Global cloud cover for assessment of optical satellite observation opportunities: A HyspIRI case study, *Remote Sensing of Environment*, *126*, 62-71, doi:10.1016/j.rse.2012.08.007.

Metelka, V., L. Baratoux, M. W. Jessell, and S. Naba (2015), Visible and infrared properties of unaltered to weathered rocks from Precambrian granite-greenstone terrains of the West African Craton, *Journal of African Earth Sciences*, *112*, 570-585, doi:10.1016/j.jafrearsci.2015.10.003.

Metternicht, G., Hurni, L., Gogu, R. (2005) Remote sensing of landslides: An analysis of the potential

contribution to geo-spatial systems for hazard assessment in mountainous environments. Remote Sensing of Environment, 98, 2-3, 284-303.

Middleton EM, Ungar SG, Mandl DJ, Ong L, Frye SW, Campbell PE, Landis DR, Young JP, Pollack NH. (2013) The earth observing one (EO-1) satellite mission: Over a decade in space. Selected Topics in Applied Earth Observations and Remote Sensing, IEEE Journal Apr;6(2):243-56.

Mouroulis, P., R. O. Green, B. Van Gorp, L. B. Moore, D. W. Wilson, H. Bender (2016): "Landsat swath imaging spectrometer design", Optical Engineering 55(1) 015104 doi:10.1117/1.OE.55.1.015104

Murchie, S., et al. (2007) Compact reconnaissance imaging spectrometer for Mars (CRISM) on Mars reconnaissance orbiter (MRO). *Journal of Geophysical Research: Planets*, 112.E5, 57 p.

Murchie, S. L., et al. (2009), A synthesis of Martian aqueous mineralogy after 1 Mars year of observations from the Mars Reconnaissance Orbiter, *Journal of Geophysical Research-Planets*, *114*, doi:10.1029/2009je003342.

NASA (2014) Strategic Plan 2014. Available on line http://science.nasa.gov/media/medialibrary/2014/04/18/FY2014_NASA_StrategicPlan_508c.pdf last accessed May 8, 2016.

NRC (2007) Earth Science and Applications from Space: National Imperatives for the Next Decade and Beyond. National Academies Press, Washington, D.C.

NRC (2010) Landscapes on the Edge: New Horizons for Research on Earth's Surface. National Academies Press, Washington, D.C.

NRC (2012) New Research Opportunities in the Earth Sciences. National Academies Press, Washington, D.C.

NRC (2013) Landsat and Beyond: Sustaining and Enhancing the Nation's Land Imaging Program, National Academies Press, Washington, D.C.

NSF Critical Zone Report (2005) Frontiers in Exploration of the Critical Zone, http://www.czen.org/sites/default/files/CZEN_Booklet.pdf

Opfergelt S, Delmelle P, Boivin P, Delvaux B (2006) The 1998 debris avalanche at Casita volcano, Nicaragua: investigation of the role of hydrothermal smectite in promoting slope instability. Geophys Res Lett 33(15):4. doi:10.1029/2006gl026661

Pieters, C. M., et al. (2011), Mg-spinel lithology: A new rock type on the lunar farside, *Journal of Geophysical Research-Planets*, *116*, doi:10.1029/2010je003727.

Riaza, A., Buzzi, J., Garcia-Melenzed, E, Carrere, V, Muller, A, (2011) Monitoring the Extent of Contamination from Acid Mine Drainage in the Iberian Pyrite Belt (SW Spain) Using Hyperspectral Imagery . Remote Sens., 3, 2166-2186, doi:10.3390/rs3102166

Rocha-Lima, A., J. V. Martins, L. A. Remer, N. A. Krotkov, M. H. Tabacniks, Y. Ben-Ami, and P.

Artaxo (2014), Optical, microphysical and compositional properties of the Eyjafjallajokull volcanic ash, *Atmospheric Chemistry and Physics*, *14*(19), 10649-10661, doi:10.5194/acp-14-10649-2014.

Rockwell, B. W., and A. H. Hofstra (2008), Identification of quartz and carbonate minerals across northern Nevada using ASTER thermal infrared emissivity data - Implications for geologic mapping and mineral resource investigations in well-studied and frontier areas, *Geosphere*, *4*(1), 218-246, doi:10.1130/ges00126.1.

Rowan, L. C., J. C. Mars, and C. J. Simpson (2005), Lithologic mapping of the Mordor, NT, Australia ultramafic complex by using the Advanced Spaceborne Thermal Emission and Reflection Radiometer (ASTER), *Remote Sensing of Environment*, *99*(1-2), 105-126, doi:10.1016/j.rse.2004.11.021.

Rowan, Lawrence C., et al. (1995) Analysis of airborne visible-infrared imaging spectrometer (AVIRIS) data of the Iron Hill, Colorado, carbonatite-alkalic igneous complex." Economic Geology 90.7: 1966-1982.

Roy, R., Launeau, P., Carrère, V., Pinet, P.C., Ceuleneer, G., Clénet, H., Daydou, Y., Girardeau, J., Amri, I., (2008) Geological mapping strategy using VNIR hyperspectral remote sensing: application to the Oman ophiolite (Sumail Massif). Geochemistry Geophysics Geosystems 10, Q02004. doi:10.1029/2008GC002154.

Sabins, Floyd F. (1999) Remote sensing for mineral exploration. Ore Geology Reviews 14.3: 157-183.

Slonecker, ET, Fischer, GB. (2014) An Evaluation of Remote Sensing Technologies for the Detection of Residual Contamination at Ready-for Anticipated Use Sites. US Geological Survey Open-File Report 2014-1197, 25p.

Soeters R. & Van Westen C.J. (1996) Slope instability, recognition, analysis and zonation. In: Turner, A. K. & Schuster R. L. (eds) Landslides: Investigation and Mitigation. Special Report, 247. Transportation Board, Washington, 129–173.

Stevens, A., Udelhoven, T., Denis, A., Tychon, B., Lioy, R., Hoffmann, L., & van Wesemael, B. (2010). Measuring soil organic carbon in croplands at regional scale using airborne imaging spectroscopy. *Geoderma, 158*, 32-45

Stevens, A., van Wesemael, B., Bartholomeus, H., Rosillon, D., Tychon, B., & Ben-Dor, E. (2008). Laboratory, field and airborne spectroscopy for monitoring organic carbon content in agricultural soils. *Geoderma, 144*, 395-404

Swayze, Gregg A., et al. (2000) Using imaging spectroscopy to map acidic mine waste." Environmental Science & Technology 34.1: 47-54.

Swayze, G. A., R. N. Clark, A. F. H. Goetz, T. G. Chrien, and N. S. Gorelick, (2003) Effects of spectrometer band pass, sampling, and signal-to-noise ratio on spectral identification using the Tetracorder algorithm, J. Geophys. Res., 108(E9), 5105, doi:10.1029/2002JE001975

Swayze, Gregg A., et al. (2009) Mapping potentially asbestos-bearing rocks using imaging spectroscopy. Geology 37.8 763-766.

Swayze, Gregg A., et al. (2014) Mapping advanced argillic alteration at Cuprite, Nevada, using imaging spectroscopy. Economic Geology 109.5: 1179-1221.

Thompson, David R., et al. (2015) Atmospheric correction for global mapping spectroscopy: ATREM advances for the HyspIRI preparatory campaign. Remote Sensing of Environment 167: 64-77.

Thompson, D., Dar A. Roberts, B.C. Gao, R.O. Green, L. Guild, K. Hayashi, R. Kudela, and S. Palacios, (2016) Atmospheric correction with the Bayesian empirical line, Opt. Express 24, 2134-2144.

Ungar, Stephen G., et al. (2003) Overview of the earth observing one (EO-1) mission. Geoscience and Remote Sensing, IEEE Transactions on 41.6: 1149-1159.

USGS (2007) Facing tomorrow's challenges—U.S. Geological Survey science in the decade 2007–2017: U.S. Geological Survey Circular 1309, x + 70 p.

Van Gorp, B., P. Mouroulis, D. W. Wilson, R. O. Green, (2014) Design of the Compact Wide Swath Imaging Spectrometer (CWIS), Proc. SPIE 9222, 92220C, doi:10.1117/12.2062886

Vane, Gregg, Alexander FH Goetz, and John B. Wellman. (1984) Airborne imaging spectrometer: A new tool for remote sensing. Geoscience and Remote Sensing, IEEE Transactions on 6: 546-549.

Whiting, M.L., Ustin, S.L., Zarco-Tejada, P., Palacios-Orueta, A., & Vanderbilt, V.C. (2006). Hyperspectral mapping of crop and soils for precision agriculture. In Remote Sensing and Modeling of Ecosystems for Sustainability III, edited by Wei Gao, Susan L. Ustin,
Proc. of SPIE Vol. 6298, 62980B, 15 p., doi: 10.1117/12.681289.

Whitworth, MCZ, Giles, D.P, Murphy, W. (2005)Airborne remote sensing for landslide hazard assessment: a case study on the Jurassic escarpment slopes of Worcestershire, UK. Quarterly Journal of Engineering Geology and Hydrogeology, 38, 285–300.

Wright, R., H. Garbeil, and A. J. L. Harris (2008) Using infrared satellite data to drive a thermo-rheological/stochastic lava flow emplacement model: A method for near-real-time volcanic hazard assessment, *Geophysical Research Letters*, *35*(19), doi:10.1029/2008gl035228.